

# Colour reconnection studies in $e^+e^- \rightarrow W^+W^-$ at $\sqrt{s} = 183$ GeV

The OPAL Collaboration

Abstract

The predicted effects of final state interactions such as colour reconnection are investigated by measuring properties of hadronic decays of W bosons, recorded at a centre-of-mass energy of  $\sqrt{s} \simeq 182.7$  GeV in the OPAL detector at LEP. Dependence on the modelling of hadronic W decays is avoided by comparing  $W^+W^- \rightarrow q\bar{q}'q\bar{q}'$  events with the non-leptonic component of  $W^+W^- \rightarrow q\bar{q}'\ell\bar{\nu}_\ell$  events. The scaled momentum distribution, its mean value,  $\langle x_p \rangle$ , and that of the charged particle multiplicity,  $\langle n_{\text{ch}} \rangle$ , are measured and found to be consistent in the two channels. The measured differences are:

$$\begin{aligned}\Delta\langle n_{\text{ch}} \rangle &= \langle n_{\text{ch}}^{4q} \rangle - 2\langle n_{\text{ch}}^{qq\ell\nu} \rangle = +0.7 \pm 0.8 \pm 0.6 \\ \Delta\langle x_p \rangle &= \langle x_p^{4q} \rangle - \langle x_p^{qq\ell\nu} \rangle = (-0.09 \pm 0.09 \pm 0.05) \times 10^{-2}.\end{aligned}$$

In addition, measurements of rapidity and thrust are performed for  $W^+W^- \rightarrow q\bar{q}'q\bar{q}'$  events. The data are described well by standard QCD models and disfavour one model of colour reconnection within the ARIADNE program. The current implementation of the Ellis-Geiger model of colour reconnection is excluded. At the current level of statistical precision no evidence for colour reconnection effects was found in the observables studied. The predicted effect of colour reconnection on OPAL measurements of  $M_W$  is also quantified in the context of models studied.

(Submitted to Physics Letters **B**)

# The OPAL Collaboration

G. Abbiendi<sup>2</sup>, K. Ackerstaff<sup>8</sup>, G. Alexander<sup>23</sup>, J. Allison<sup>16</sup>, N. Altekamp<sup>5</sup>, K.J. Anderson<sup>9</sup>,  
S. Anderson<sup>12</sup>, S. Arcelli<sup>17</sup>, S. Asai<sup>24</sup>, S.F. Ashby<sup>1</sup>, D. Axen<sup>29</sup>, G. Azuelos<sup>18,a</sup>, A.H. Ball<sup>17</sup>,  
E. Barberio<sup>8</sup>, R.J. Barlow<sup>16</sup>, R. Bartoldus<sup>3</sup>, J.R. Batley<sup>5</sup>, S. Baumann<sup>3</sup>, J. Bechtluft<sup>14</sup>, T. Behnke<sup>27</sup>,  
K.W. Bell<sup>20</sup>, G. Bella<sup>23</sup>, A. Bellerive<sup>9</sup>, S. Bentvelsen<sup>8</sup>, S. Bethke<sup>14</sup>, S. Betts<sup>15</sup>, O. Biebel<sup>14</sup>, A. Biguzzi<sup>5</sup>,  
S.D. Bird<sup>16</sup>, V. Blobel<sup>27</sup>, I.J. Bloodworth<sup>1</sup>, P. Bock<sup>11</sup>, J. Böhme<sup>14</sup>, D. Bonacorsi<sup>2</sup>, M. Boutemour<sup>34</sup>,  
S. Braibant<sup>8</sup>, P. Bright-Thomas<sup>1</sup>, L. Brigliadori<sup>2</sup>, R.M. Brown<sup>20</sup>, H.J. Burckhart<sup>8</sup>, P. Capiluppi<sup>2</sup>,  
R.K. Carnegie<sup>6</sup>, A.A. Carter<sup>13</sup>, J.R. Carter<sup>5</sup>, C.Y. Chang<sup>17</sup>, D.G. Charlton<sup>1,b</sup>, D. Chrisman<sup>4</sup>,  
C. Ciocca<sup>2</sup>, P.E.L. Clarke<sup>15</sup>, E. Clay<sup>15</sup>, I. Cohen<sup>23</sup>, J.E. Conboy<sup>15</sup>, O.C. Cooke<sup>8</sup>, C. Couyoumtzelis<sup>13</sup>,  
R.L. Coxe<sup>9</sup>, M. Cuffiani<sup>2</sup>, S. Dado<sup>22</sup>, G.M. Dallavalle<sup>2</sup>, R. Davis<sup>30</sup>, S. De Jong<sup>12</sup>, A. de Roeck<sup>8</sup>,  
P. Dervan<sup>15</sup>, K. Desch<sup>8</sup>, B. Dienes<sup>33,d</sup>, M.S. Dixit<sup>7</sup>, J. Dubbert<sup>34</sup>, E. Duchovni<sup>26</sup>, G. Duckeck<sup>34</sup>,  
I.P. Duerdoth<sup>16</sup>, D. Eatough<sup>16</sup>, P.G. Estabrooks<sup>6</sup>, E. Etzion<sup>23</sup>, F. Fabbri<sup>2</sup>, M. Fantì<sup>2</sup>, A.A. Faust<sup>30</sup>,  
F. Fiedler<sup>27</sup>, M. Fierro<sup>2</sup>, I. Fleck<sup>8</sup>, R. Folman<sup>26</sup>, A. Fürtjes<sup>8</sup>, D.I. Futyan<sup>16</sup>, P. Gagnon<sup>7</sup>, J.W. Gary<sup>4</sup>,  
J. Gascon<sup>18</sup>, S.M. Gascon-Shotkin<sup>17</sup>, G. Gaycken<sup>27</sup>, C. Geich-Gimbel<sup>3</sup>, G. Giacomelli<sup>2</sup>, P. Giacomelli<sup>2</sup>,  
V. Gibson<sup>5</sup>, W.R. Gibson<sup>13</sup>, D.M. Gingrich<sup>30,a</sup>, D. Glenzinski<sup>9</sup>, J. Goldberg<sup>22</sup>, W. Gorn<sup>4</sup>, C. Grandi<sup>2</sup>,  
K. Graham<sup>28</sup>, E. Gross<sup>26</sup>, J. Grunhaus<sup>23</sup>, M. Gruwe<sup>27</sup>, G.G. Hanson<sup>12</sup>, M. Hansroul<sup>8</sup>, M. Hapke<sup>13</sup>,  
K. Harder<sup>27</sup>, A. Harel<sup>22</sup>, C.K. Hargrove<sup>7</sup>, C. Hartmann<sup>3</sup>, M. Hauschild<sup>8</sup>, C.M. Hawkes<sup>1</sup>,  
R. Hawkings<sup>27</sup>, R.J. Hemingway<sup>6</sup>, M. Herndon<sup>17</sup>, G. Herten<sup>10</sup>, R.D. Heuer<sup>27</sup>, M.D. Hildreth<sup>8</sup>,  
J.C. Hill<sup>5</sup>, P.R. Hobson<sup>25</sup>, M. Hoch<sup>18</sup>, A. Hocker<sup>9</sup>, K. Hoffman<sup>8</sup>, R.J. Homer<sup>1</sup>, A.K. Honma<sup>28,a</sup>,  
D. Horváth<sup>32,c</sup>, K.R. Hossain<sup>30</sup>, R. Howard<sup>29</sup>, P. Hüntemeyer<sup>27</sup>, P. Igo-Kemenes<sup>11</sup>, D.C. Imrie<sup>25</sup>,  
K. Ishii<sup>24</sup>, F.R. Jacob<sup>20</sup>, A. Jawahery<sup>17</sup>, H. Jeremie<sup>18</sup>, M. Jimack<sup>1</sup>, C.R. Jones<sup>5</sup>, P. Jovanovic<sup>1</sup>,  
T.R. Junk<sup>6</sup>, D. Karlen<sup>6</sup>, V. Kartvelishvili<sup>16</sup>, K. Kawagoe<sup>24</sup>, T. Kawamoto<sup>24</sup>, P.I. Kayal<sup>30</sup>,  
R.K. Keeler<sup>28</sup>, R.G. Kellogg<sup>17</sup>, B.W. Kennedy<sup>20</sup>, D.H. Kim<sup>19</sup>, A. Klier<sup>26</sup>, S. Kluth<sup>8</sup>, T. Kobayashi<sup>24</sup>,  
M. Kobel<sup>3,e</sup>, D.S. Koetke<sup>6</sup>, T.P. Kokott<sup>3</sup>, M. Kolrep<sup>10</sup>, S. Komamiya<sup>24</sup>, R.V. Kowalewski<sup>28</sup>, T. Kress<sup>4</sup>,  
P. Krieger<sup>6</sup>, J. von Krogh<sup>11</sup>, T. Kuhl<sup>3</sup>, P. Kyberd<sup>13</sup>, G.D. Lafferty<sup>16</sup>, H. Landsman<sup>22</sup>, D. Lanske<sup>14</sup>,  
J. Lauber<sup>15</sup>, S.R. Lautenschlager<sup>31</sup>, I. Lawson<sup>28</sup>, J.G. Layter<sup>4</sup>, D. Lazic<sup>22</sup>, A.M. Lee<sup>31</sup>, D. Lellouch<sup>26</sup>,  
J. Letts<sup>12</sup>, L. Levinson<sup>26</sup>, R. Liebis<sup>11</sup>, B. List<sup>8</sup>, C. Littlewood<sup>5</sup>, A.W. Lloyd<sup>1</sup>, S.L. Lloyd<sup>13</sup>,  
F.K. Loebinger<sup>16</sup>, G.D. Long<sup>28</sup>, M.J. Losty<sup>7</sup>, J. Ludwig<sup>10</sup>, D. Liu<sup>12</sup>, A. Macchiolo<sup>2</sup>, A. Macpherson<sup>30</sup>,  
W. Mader<sup>3</sup>, M. Mannelli<sup>8</sup>, S. Marcellini<sup>2</sup>, C. Markopoulos<sup>13</sup>, A.J. Martin<sup>13</sup>, J.P. Martin<sup>18</sup>,  
G. Martinez<sup>17</sup>, T. Mashimo<sup>24</sup>, P. Mättig<sup>26</sup>, W.J. McDonald<sup>30</sup>, J. McKenna<sup>29</sup>, E.A. Mckigney<sup>15</sup>,  
T.J. McMahon<sup>1</sup>, R.A. McPherson<sup>28</sup>, F. Meijers<sup>8</sup>, S. Menke<sup>3</sup>, F.S. Merritt<sup>9</sup>, H. Mes<sup>7</sup>, J. Meyer<sup>27</sup>,  
A. Michelini<sup>2</sup>, S. Mihara<sup>24</sup>, G. Mikenberg<sup>26</sup>, D.J. Miller<sup>15</sup>, R. Mir<sup>26</sup>, W. Mohr<sup>10</sup>, A. Montanari<sup>2</sup>,  
T. Mori<sup>24</sup>, K. Nagai<sup>8</sup>, I. Nakamura<sup>24</sup>, H.A. Neal<sup>12</sup>, B. Nellen<sup>3</sup>, R. Nisius<sup>8</sup>, S.W. O’Neale<sup>1</sup>,  
F.G. Oakham<sup>7</sup>, F. Odorici<sup>2</sup>, H.O. Ogren<sup>12</sup>, M.J. Oreglia<sup>9</sup>, S. Orito<sup>24</sup>, J. Pálinkás<sup>33,d</sup>, G. Pásztor<sup>32</sup>,  
J.R. Pater<sup>16</sup>, G.N. Patrick<sup>20</sup>, J. Patt<sup>10</sup>, R. Perez-Ochoa<sup>8</sup>, S. Petzold<sup>27</sup>, P. Pfeifenschneider<sup>14</sup>,  
J.E. Pilcher<sup>9</sup>, J. Pinfold<sup>30</sup>, D.E. Plane<sup>8</sup>, P. Poffenberger<sup>28</sup>, J. Polok<sup>8</sup>, M. Przybycień<sup>8</sup>, C. Rembser<sup>8</sup>,  
H. Rick<sup>8</sup>, S. Robertson<sup>28</sup>, S.A. Robins<sup>22</sup>, N. Rodning<sup>30</sup>, J.M. Roney<sup>28</sup>, K. Roscoe<sup>16</sup>, A.M. Rossi<sup>2</sup>,  
Y. Rozen<sup>22</sup>, K. Runge<sup>10</sup>, O. Runolfsson<sup>8</sup>, D.R. Rust<sup>12</sup>, K. Sachs<sup>10</sup>, T. Saeki<sup>24</sup>, O. Sahr<sup>34</sup>, W.M. Sang<sup>25</sup>,  
E.K.G. Sarkisyan<sup>23</sup>, C. Sbarra<sup>29</sup>, A.D. Schaile<sup>34</sup>, O. Schaile<sup>34</sup>, F. Scharf<sup>3</sup>, P. Scharff-Hansen<sup>8</sup>,  
J. Schieck<sup>11</sup>, B. Schmitt<sup>8</sup>, S. Schmitt<sup>11</sup>, A. Schöning<sup>8</sup>, M. Schröder<sup>8</sup>, M. Schumacher<sup>3</sup>, C. Schwick<sup>8</sup>,  
W.G. Scott<sup>20</sup>, R. Seuster<sup>14</sup>, T.G. Shears<sup>8</sup>, B.C. Shen<sup>4</sup>, C.H. Shepherd-Themistocleous<sup>8</sup>, P. Sherwood<sup>15</sup>,  
G.P. Siroli<sup>2</sup>, A. Sittler<sup>27</sup>, A. Skuja<sup>17</sup>, A.M. Smith<sup>8</sup>, G.A. Snow<sup>17</sup>, R. Sobie<sup>28</sup>, S. Söldner-Rembold<sup>10</sup>,  
S. Spagnolo<sup>20</sup>, M. Sproston<sup>20</sup>, A. Stahl<sup>3</sup>, K. Stephens<sup>16</sup>, J. Steuerer<sup>27</sup>, K. Stoll<sup>10</sup>, D. Strom<sup>19</sup>,  
R. Ströhmer<sup>34</sup>, B. Surrow<sup>8</sup>, S.D. Talbot<sup>1</sup>, P. Taras<sup>18</sup>, S. Tarem<sup>22</sup>, R. Teuscher<sup>8</sup>, M. Thiergen<sup>10</sup>,  
J. Thomas<sup>15</sup>, M.A. Thomson<sup>8</sup>, E. von Törne<sup>3</sup>, E. Torrence<sup>8</sup>, S. Towers<sup>6</sup>, I. Trigger<sup>18</sup>, Z. Trócsányi<sup>33</sup>,  
E. Tsur<sup>23</sup>, A.S. Turcot<sup>9</sup>, M.F. Turner-Watson<sup>1</sup>, I. Ueda<sup>24</sup>, R. Van Kooten<sup>12</sup>, P. Vannerem<sup>10</sup>,  
M. Verzocchi<sup>10</sup>, H. Voss<sup>3</sup>, F. Wackerle<sup>10</sup>, A. Wagner<sup>27</sup>, C.P. Ward<sup>5</sup>, D.R. Ward<sup>5</sup>, P.M. Watkins<sup>1</sup>,  
A.T. Watson<sup>1</sup>, N.K. Watson<sup>1</sup>, P.S. Wells<sup>8</sup>, N. Vermes<sup>3</sup>, J.S. White<sup>6</sup>, G.W. Wilson<sup>16</sup>, J.A. Wilson<sup>1</sup>,  
T.R. Wyatt<sup>16</sup>, S. Yamashita<sup>24</sup>, G. Yekutieli<sup>26</sup>, V. Zacek<sup>18</sup>, D. Zer-Zion<sup>8</sup>

- <sup>1</sup>School of Physics and Astronomy, University of Birmingham, Birmingham B15 2TT, UK
- <sup>2</sup>Dipartimento di Fisica dell' Università di Bologna and INFN, I-40126 Bologna, Italy
- <sup>3</sup>Physikalisches Institut, Universität Bonn, D-53115 Bonn, Germany
- <sup>4</sup>Department of Physics, University of California, Riverside CA 92521, USA
- <sup>5</sup>Cavendish Laboratory, Cambridge CB3 0HE, UK
- <sup>6</sup>Ottawa-Carleton Institute for Physics, Department of Physics, Carleton University, Ottawa, Ontario K1S 5B6, Canada
- <sup>7</sup>Centre for Research in Particle Physics, Carleton University, Ottawa, Ontario K1S 5B6, Canada
- <sup>8</sup>CERN, European Organisation for Particle Physics, CH-1211 Geneva 23, Switzerland
- <sup>9</sup>Enrico Fermi Institute and Department of Physics, University of Chicago, Chicago IL 60637, USA
- <sup>10</sup>Fakultät für Physik, Albert Ludwigs Universität, D-79104 Freiburg, Germany
- <sup>11</sup>Physikalisches Institut, Universität Heidelberg, D-69120 Heidelberg, Germany
- <sup>12</sup>Indiana University, Department of Physics, Swain Hall West 117, Bloomington IN 47405, USA
- <sup>13</sup>Queen Mary and Westfield College, University of London, London E1 4NS, UK
- <sup>14</sup>Technische Hochschule Aachen, III Physikalisches Institut, Sommerfeldstrasse 26-28, D-52056 Aachen, Germany
- <sup>15</sup>University College London, London WC1E 6BT, UK
- <sup>16</sup>Department of Physics, Schuster Laboratory, The University, Manchester M13 9PL, UK
- <sup>17</sup>Department of Physics, University of Maryland, College Park, MD 20742, USA
- <sup>18</sup>Laboratoire de Physique Nucléaire, Université de Montréal, Montréal, Quebec H3C 3J7, Canada
- <sup>19</sup>University of Oregon, Department of Physics, Eugene OR 97403, USA
- <sup>20</sup>CLRC Rutherford Appleton Laboratory, Chilton, Didcot, Oxfordshire OX11 0QX, UK
- <sup>22</sup>Department of Physics, Technion-Israel Institute of Technology, Haifa 32000, Israel
- <sup>23</sup>Department of Physics and Astronomy, Tel Aviv University, Tel Aviv 69978, Israel
- <sup>24</sup>International Centre for Elementary Particle Physics and Department of Physics, University of Tokyo, Tokyo 113-0033, and Kobe University, Kobe 657-8501, Japan
- <sup>25</sup>Institute of Physical and Environmental Sciences, Brunel University, Uxbridge, Middlesex UB8 3PH, UK
- <sup>26</sup>Particle Physics Department, Weizmann Institute of Science, Rehovot 76100, Israel
- <sup>27</sup>Universität Hamburg/DESY, II Institut für Experimental Physik, Notkestrasse 85, D-22607 Hamburg, Germany
- <sup>28</sup>University of Victoria, Department of Physics, P O Box 3055, Victoria BC V8W 3P6, Canada
- <sup>29</sup>University of British Columbia, Department of Physics, Vancouver BC V6T 1Z1, Canada
- <sup>30</sup>University of Alberta, Department of Physics, Edmonton AB T6G 2J1, Canada
- <sup>31</sup>Duke University, Dept of Physics, Durham, NC 27708-0305, USA
- <sup>32</sup>Research Institute for Particle and Nuclear Physics, H-1525 Budapest, P O Box 49, Hungary
- <sup>33</sup>Institute of Nuclear Research, H-4001 Debrecen, P O Box 51, Hungary
- <sup>34</sup>Ludwigs-Maximilians-Universität München, Sektion Physik, Am Coulombwall 1, D-85748 Garching, Germany

<sup>a</sup> and at TRIUMF, Vancouver, Canada V6T 2A3

<sup>b</sup> and Royal Society University Research Fellow

<sup>c</sup> and Institute of Nuclear Research, Debrecen, Hungary

<sup>d</sup> and Department of Experimental Physics, Lajos Kossuth University, Debrecen, Hungary

<sup>e</sup> on leave of absence from the University of Freiburg

# 1 Introduction

Hadronic data in  $e^+e^-$  collisions can be characterised by event shape distributions and inclusive observables such as charged particle multiplicities and momentum spectra. In addition to tests of Monte Carlo models, measurement of the properties of the hadronic sector of  $W^+W^-$  decays allows the question of “colour reconnection” [1] to be addressed experimentally. The decay products of the two  $W$  decays may have a significant space-time overlap as the separation of their decay vertices at LEP2 energies is small compared to characteristic hadronic distance scales. In the fully hadronic channel this may lead to new types of final state interactions. Colour reconnection is the general name applied to the case where such final state interactions lead to colour flow between the decay products of the two  $W$  bosons. At present there is general consensus that observable effects of such interactions during the perturbative phase are expected to be small [2]. In contrast, significant interference in the hadronisation process is considered to be a real possibility. With the current knowledge of non-perturbative QCD, such interference can be estimated only in the context of specific models [1–9]. One should be aware that other final state effects such as Bose-Einstein correlations between identical bosons may also influence the observed event properties.

It has been suggested [2, 4] that simple observable quantities, such as the charged multiplicity in restricted rapidity intervals, may be particularly sensitive to the effects of colour reconnection. Later studies [10, 11] showed that the initial estimates of [4] were incorrect for a variety of reasons<sup>1</sup>. More recently, studies using the Ellis-Geiger model [8, 9] suggested that the effect on the inclusive charged multiplicity itself may be larger than previously considered and that the mean hadronic multiplicity in  $W^+W^- \rightarrow q\bar{q}'q\bar{q}'$  events,  $\langle n_{\text{ch}}^{4q} \rangle$ , may be as much as 10% smaller than twice the hadronic multiplicity in  $W^+W^- \rightarrow q\bar{q}'\ell\bar{\nu}_\ell$  events,  $\langle n_{\text{ch}}^{\text{qq}\ell\nu} \rangle$  [12]. The visible effects of such phenomena are expected to manifest themselves most clearly for low momentum particles, e.g. as illustrated in [11]. Therefore, studies of the fragmentation function, i.e. the distribution of the scaled momentum,  $x_p = p/E_{\text{beam}}$ , are also relevant. The shape of a charged particle multiplicity distribution may be quantified by its dispersion (r.m.s.),  $D$ , and so  $D^{4q}$  and  $D^{\text{qq}\ell\nu}$  are measured.

Some earlier estimates of the sensitivity to colour reconnection have been made within the context of given models, comparing “reconnection” to “no reconnection” scenarios for  $W^+W^- \rightarrow q\bar{q}'q\bar{q}'$  events. In general, both the size and sign of any changes are dependent upon the model considered. At the expense of a reduction in statistical sensitivity, the dependence on the modelling of single hadronic  $W$  decays can be avoided by comparing directly the properties of the hadronic part of  $W^+W^- \rightarrow q\bar{q}'\ell\bar{\nu}_\ell$  events with  $W^+W^- \rightarrow q\bar{q}'q\bar{q}'$  events. In the current study, the inclusive charged particle multiplicity and the fragmentation function are measured for  $W^+W^- \rightarrow q\bar{q}'q\bar{q}'$  and the non-leptonic component of  $W^+W^- \rightarrow q\bar{q}'\ell\bar{\nu}_\ell$  events. Charged particles associated with the leptonically decaying  $W$  are excluded from these measurements. The quantities  $\Delta\langle n_{\text{ch}} \rangle = \langle n_{\text{ch}}^{4q} \rangle - 2\langle n_{\text{ch}}^{\text{qq}\ell\nu} \rangle$ ,  $\Delta D = D^{4q} - \sqrt{2}D^{\text{qq}\ell\nu}$  and  $\Delta\langle x_p \rangle = \langle x_p^{4q} \rangle - \langle x_p^{\text{qq}\ell\nu} \rangle$  are examined. The mean values of the thrust distribution,  $\langle 1 - T^{4q} \rangle$ , and the rapidity distribution relative to the thrust axis,  $\langle |y^{4q}| \rangle$ , are measured to characterise the global properties of  $W^+W^- \rightarrow q\bar{q}'q\bar{q}'$  events themselves. These are not expected to be particularly sensitive to the effects of colour reconnection [2].

Models of colour reconnection as implemented in the event generators PYTHIA (Sjöstrand-Khoze model [2]), ARIADNE (model [5]) and HERWIG (model [7, 13]) have been used in previous studies to assess the sensitivities of the quantities above [11]. The models ARIADNE and a “colour octet” variant<sup>2</sup> of HERWIG [14] predicted shifts in  $\langle n_{\text{ch}}^{4q} \rangle$  and  $\langle x_p^{4q} \rangle$  similar in size to the expected statistical uncertainty

<sup>1</sup>The dominant effect was to have neglected the polarisation of the  $W$ .

<sup>2</sup>Merging of partons to form clusters was performed on a nearest neighbour basis, as a partial emulation of the model of Reference [8].

on these quantities using the data studied in this letter. However, in the studies of [11] no additional retuning of the models was performed after reconnection effects were included.

In this letter, emphasis is placed on predictions from reconnection models which have been suitably tuned to describe  $Z^0$  data. The predictions from the reconnection models of ARIADNE, Sjöstrand-Khoze, and Ellis-Geiger are considered, where the tuning of these models is summarised in Section 4. The version of HERWIG including reconnection effects has not yet been tuned by OPAL and is therefore not discussed further herein.

## 2 Data Selection

This analysis uses data recorded during 1997 by the OPAL detector, which is described fully elsewhere [15]. The measurement of luminosity is identical to that in [16]. The integrated luminosity used in this analysis is  $57.21 \pm 0.15(\text{stat.}) \pm 0.20(\text{syst.}) \text{ pb}^{-1}$  at a luminosity weighted mean centre-of-mass energy of  $\sqrt{s} = 182.68 \pm 0.05 \text{ GeV}$  [17].

Events are selected in the  $W^+W^- \rightarrow q\bar{q}'\ell\bar{\nu}_\ell$  and  $W^+W^- \rightarrow q\bar{q}'q\bar{q}'$  channels using the likelihood selections described in [18,19]. In total, 433  $W^+W^- \rightarrow q\bar{q}'q\bar{q}'$  and 361  $W^+W^- \rightarrow q\bar{q}'\ell\bar{\nu}_\ell$  candidates are selected. The Monte Carlo models without colour reconnection and the detector simulation are identical to those in [19]. The models of colour reconnection studied are described in Section 4.

Charged particles may have up to 159 hits in the jet chamber. Tracks used in the analysis are required to have a minimum of 40 hits in the  $|\cos\theta|$  region<sup>3</sup> in which at least 80 are possible. At larger  $|\cos\theta|$ , the number of hits is required to be greater than 50% of the expected number and also greater than 20. Tracks must have a momentum component in the plane perpendicular to the beam axis of greater than 0.15 GeV/ $c$ , and a measured momentum of less than 100 GeV/ $c$ . The extrapolated point of closest approach of each track to the interaction point is required to be less than 2 cm in the  $r$ - $\phi$  plane and less than 25 cm in  $z$ . Clusters of energy in the electromagnetic calorimeter were required to have a measured energy greater than 0.10 GeV (0.25 GeV) if they occurred in the barrel (endcap) region of the detector.

## 3 Data Analysis and Correction Procedure

The analysis of the event properties follows the unfolding procedure described in [18]. The distributions of  $n_{\text{ch}}$ ,  $x_p$ ,  $1 - T$  and  $y$  are corrected for background contamination using a bin-by-bin subtraction of the expected background, based on Monte Carlo estimates. Corrections (described below) are then applied for finite acceptance and the effects of detector resolution, after which mean values of the distributions are calculated. Each observable is evaluated using two samples of  $e^+e^- \rightarrow W^+W^-$  events generated using the KORALW [20] Monte Carlo program. The first, which includes initial state radiation and a full simulation of the OPAL detector, contains only those events which pass the cuts applied to the data (detector level). The second does not include initial state radiation or detector effects and allows all particles with lifetimes shorter than  $3 \times 10^{-10} \text{ s}$  to decay (hadron level). Both samples are generated at the same  $\sqrt{s}$ . Distributions normalised to the number of events at the detector and the hadron level are compared to derive bin-by-bin correction factors which are used to

---

<sup>3</sup>The OPAL coordinate system is defined such that the origin is at the geometric centre of the jet chamber,  $z$  is parallel to, and has positive sense along, the  $e^-$  beam direction,  $r$  is the coordinate normal to  $z$ ,  $\theta$  is the polar angle with respect to  $+z$  and  $\phi$  is the azimuthal angle around  $z$ .

correct the observed distributions of  $x_p$ ,  $1 - T$  and  $y$  to the hadron level. In contrast to the other observables which are formed from charged particles alone, thrust is measured using both charged particles and clusters of electromagnetic energy unassociated with charged particles.

A bin-by-bin correction procedure is suitable for the quantities above as the effects of finite resolution and acceptance do not cause significant migration (and therefore correlation) between bins. Such a method is not readily applicable to multiplicity distributions, due to the large correlations between bins. Instead, a matrix correction is used to correct for detector resolution effects, followed by a bin-by-bin correction which accounts for the residual effects due to acceptance cuts and initial state radiation, as in previous OPAL multiplicity studies [21].

The uncorrected multiplicity distributions for the  $W^+W^-$  candidate events before background subtraction are illustrated in Figure 1, together with the predictions of Monte Carlo events without colour reconnection, but including detector simulation. The background prediction is the sum of all Standard Model processes, as described by the models used in [22]. In general, good agreement is seen between the data and predictions from the models. HERWIG predicts visibly lower charged particle multiplicities than the other models, for example almost two units lower than that of KORALW for  $W^+W^- \rightarrow q\bar{q}'q\bar{q}'$  events. This is a consequence of the poor modelling of the multiplicity difference between quark flavours in the OPAL tuning of HERWIG to  $Z^0$  data, and of the negligible b quark content of W decays.

## 4 Colour Reconnection Models

Variants of three models of colour reconnection have been investigated. The Sjöstrand-Khoze (SK) models are based upon the Lund string picture of colour confinement, in which a string is created that spans the decay product partons associated with each W. These strings expand from the respective decay vertices and subsequently fragment to hadrons. Before this occurs, at most one reconnection is allowed between sections of the two strings. The main scenarios considered are called type I and type II in analogy to the two types of superconducting vortices which could correspond to colour strings. In the SK I scenario, the two colour flux tubes have a lateral extent comparable to hadronic dimensions. The probability for reconnection to occur is proportional to the integrated space-time volume over which the two tubes cross, where a (free) strength parameter,  $\rho$ , determines the absolute normalisation. In the SK II scenario, the strings have infinitesimally small radii and a unit reconnection probability upon their first crossing. A third scenario considered, SK II', is similar to SK II but reconnection is only allowed to occur at the first string crossing which would reduce the total string length of the system. As described in [23], the only tuning necessary for these models is to ensure that the JETSET hadronisation model gives a good description of  $Z^0$  data. Therefore, the same parameters were used as for the corresponding sample of non-reconnected  $e^+e^- \rightarrow W^+W^-$  events, which for the Sjöstrand-Khoze models are generated using PYTHIA. The fractions of  $W^+W^- \rightarrow q\bar{q}'q\bar{q}'$  events in which reconnection occurs at  $\sqrt{s} = 183$  GeV are found to be 37.9% for SK I (using<sup>4</sup>  $\rho = 0.9$ ), 22.1% for SK II and 19.8% for SK II'.

The second set of two models is incorporated into the ARIADNE Monte Carlo program by its author. They may be considered as extensions of the earlier model<sup>5</sup> by Gustafson and Häkkinen [4], as both models were implemented using the ARIADNE Monte Carlo program and the same criterion

<sup>4</sup>  $\rho = 0.4$  results in a similar reconnection probability to the SK II model. The value used here increases the sensitivity of the data available by enhancing the effects of reconnection predicted by SK I.

<sup>5</sup>In [4], at most one reconnection was allowed per event and possible reconstructions within a single W were not implemented.

is employed in the reconnection ansatz to determine whether reconnection is allowed. Perturbative QCD favours configurations with minimal string length in hadronic  $Z^0$  decays [24]. When the partons of two W bosons are separating and strings formed between them, it is plausible that configurations corresponding to a reduced total string length are favoured. In the reconnection model of ARIADNE, the string length is defined in terms of the  $\Lambda$  measure, which may be viewed as the rapidity range along the string:  $\Lambda = \sum_i \ln(m_i^2/m_\rho^2)$ , where  $m_i$  is the invariant mass of string segment  $i$  and  $m_\rho$  sets a typical hadronic mass scale. Reconnections are allowed, within constraints of colour algebra factors, which lead to a reduction in the total  $\Lambda$  of the system. The first ARIADNE model considered, referred to herein as AR 2, restricts reconnections to gluons having energies less than  $\Gamma_W$ , while the second ARIADNE model, AR 3, does not impose such a restriction. As gluons emitted with energies  $> \Gamma_W \sim 2$  GeV are perturbative in nature and have been shown to be radiated incoherently by the two initial colour dipoles [2], the model AR 3 is disfavoured on theoretical grounds. Multiple reconnections per event are permitted and reconnection may occur within different string segments of the same W boson. The tuning of the models to describe  $Z^0$  data is as given in [25], with the following changes to the “ $a$ ” parameter, MSTJ(41), which governs the hardness of the fragmentation function: non-reconnected ARIADNE:  $a = 0.52$ , AR 2:  $a = 0.65$ , AR 3:  $a = 0.58$ . The fractions of  $W^+W^- \rightarrow q\bar{q}'q\bar{q}'$  events in which reconnection occurs at  $\sqrt{s} = 183$  GeV are found to be 51.9% for AR 2 and 63.4% for AR 3.

The third class of models considered is that of Ellis and Geiger [8], as implemented in the VNI Monte Carlo [9], version 4.12. This model has been used to predict relatively large changes in observables such as the mean charged particle multiplicity [12], but has so far not been subjected to significant comparison with  $W^+W^-$  data. This model has three variants, called “colour blind”, “colour singlet” and “colourful”. In the colour blind scenario, colour degrees of freedom are ignored and cluster formation from partons proceeds solely on a nearest neighbour basis in space-time. The colour singlet case requires the colour degrees of freedom of two partons to add up to a colour singlet before cluster formation may take place. In the colourful variant, partons which are not in a relative colour singlet state are also allowed to merge with each other, with the net colour degrees of freedom being balanced by the emission of additional, coloured partons. Predictions presented using this model correspond to the colour blind and colour singlet cases. Predictions from the colourful case are not shown due to technical problems. To generate  $e^+e^- \rightarrow W^+W^-$  events, with the four fermions generated by PYTHIA, it was necessary to change<sup>6</sup> the default value of several program parameters. The default tuning of the model is used, with only minor modifications<sup>7</sup>. In evaluating predictions from this model, decays of  $K_S^0$ ,  $\Lambda^0$  and  $\pi^0$  were included for consistency with the definition of stable particles given in Section 3 (not the default for VNI). Significant energy imbalances were observed in hadronic  $W^+W^-$  final states when comparing the generated particle spectra to the collision energy of 183 GeV: approximately 3% of  $W^+W^- \rightarrow q\bar{q}'q\bar{q}'$  events differed from 183 GeV by more than 0.5 GeV, while approximately 3% of  $W^+W^- \rightarrow q\bar{q}'\ell\bar{\nu}_\ell$  events had deviations of more than 20 GeV. These imbalances are unrelated to changes in the program parameters.

Results obtained using the Ellis-Geiger model in VNI are found to be rather different to those of [8, 12]. Differences predicted between the charged multiplicities in the  $W^+W^- \rightarrow q\bar{q}'q\bar{q}'$  and  $W^+W^- \rightarrow q\bar{q}'\ell\bar{\nu}_\ell$  channels are  $\sim 2\%$  of  $\langle n_{\text{ch}}^{4q} \rangle$ , with opposite signs in the colour blind and colour singlet models. It is noted that with the current version of VNI, the predicted value of  $\langle 1 - T^{4q} \rangle$  is found to be 0.30. This is considerably larger than that of 0.06 given in [8]. A small value of  $\langle 1 - T^{4q} \rangle$  indicates that an event has a two-jet like topology, allowing the hadronic showers from neighbouring W bosons to overlap, which in general is expected to enhance interconnection effects.

<sup>6</sup>MSTW(3)=2, MSTV(84)=0, 2 (blind, singlet), MSTV(16)=1, MSTV(150)=2.

<sup>7</sup>To ensure that unstable particles are decayed irrespective of their origin, and that charged particles carry a fraction of the event energy consistent with naive expectation assuming that pions dominate the final state, two changes are made: MSTV(91)=5 and MSTV(94)=0.

The Sjöstrand-Khoze, ARIADNE and Ellis-Geiger models, after simulation of the OPAL detector, are compared with the data distributions of charged particle multiplicity and thrust in the  $W^+W^- \rightarrow q\bar{q}'q\bar{q}'$  channel. Figure 2(a) presents the same data as in Figure 1(a) but compares them with the predictions of the PYTHIA and Sjöstrand-Khoze models, while Figure 2(b) compares these data with the ARIADNE and Ellis-Geiger (colour blind) models. Figure 2(c) shows the thrust distribution with a subset of these models. The model predictions are represented by smooth curves which pass through the centre of the binned predictions of each model. It can be seen that the multiplicity predicted by the Ellis-Geiger model is significantly higher than observed in data or predicted by other models studied. The same observations are made when comparing this model to  $W^+W^- \rightarrow q\bar{q}'\ell\bar{\nu}_\ell$  data. The AR 3 model predicts a charged multiplicity that is approximately 0.7 units lower than the non-reconnected ARIADNE after detector simulation. From the  $1-T$  distribution, it is noted that most models provide a good description of data, while the Ellis-Geiger model predicts events which are much more spherical. With its current implementation and tuning in the VNI program, the Ellis-Geiger model does not describe the data and is therefore not used to assess systematics on  $M_W$  (see Section 7).

## 5 Systematic Uncertainties

A number of systematic uncertainties have been considered in the analysis, as summarised in Tables 1 and 2. Each systematic uncertainty is taken as a symmetric error and the total uncertainty is defined by adding the individual contributions in quadrature. Correlations are explicitly accounted for in estimating systematic uncertainties for  $\Delta\langle n_{\text{ch}} \rangle$ ,  $\Delta\langle x_p \rangle$  and  $\Delta D$ . The dependence of the correction procedure on the Monte Carlo model is evaluated by comparing results obtained using KORALW, PYTHIA and EXCALIBUR [26] as the  $W^+W^-$  signal samples, each using the same tuning of the JETSET [3] hadronisation model. The same treatment is applied to estimate model dependence in the subtraction of the small ( $< \mathcal{O}(1\%)$ )  $W^+W^-$  background contamination in each channel:  $W^+W^- \rightarrow q\bar{q}'q\bar{q}'$  or  $W^+W^- \rightarrow \ell^+\nu_\ell\ell'^-\bar{\nu}_{\ell'}$  events selected as  $W^+W^- \rightarrow q\bar{q}'\ell\bar{\nu}_\ell$ , for example. The  $W^+W^-$  cross-section obtained from GENTLE [27] was allowed to vary from its central value of 15.71 pb by  $\pm 4.3\%$ , corresponding to the combined statistical and systematic uncertainty on the measured cross-section [19].

Hadronisation effects are estimated in a similar manner, unfolding data using HERWIG and ARIADNE,<sup>8</sup> and also each of the variants of the Sjöstrand-Khoze and ARIADNE colour reconnection models. The largest variation in any of these seven unfolding tests, dominated by the AR 3 and HERWIG models, was taken as the systematic uncertainty associated with hadronisation effects. The Ellis-Geiger model was not used for unfolding as it does not describe the observed  $W^+W^-$  data.

Uncertainties arising from the selection of charged tracks are estimated by varying the track selection cuts and repeating the analysis. The maximum allowed values of the distances of closest approach to the interaction region in  $r$ - $\phi$  and  $z$  are varied from 2 cm to 5 cm and from 25 cm to 50 cm, respectively, and the minimum number of hits on tracks is varied from 20 to 40. The dependence on charged track quality cuts is the sum in quadrature of these three effects.

The dependence on the modelling of the accepted background is the sum in quadrature of two components, accounting separately for uncertainties in normalisation and shape. Normalisation dependence is estimated by taking the largest effect observed when scaling various backgrounds before subtraction from the data. The scale factors applied, taken from the uncertainties estimated in [19], are approximately  $\pm 10\%$  for the total background in the  $q\bar{q}'q\bar{q}'$  channel and  $\pm 8\%$  in the  $q\bar{q}'\ell\bar{\nu}_\ell$  channel, and approximately  $\pm 11\%$  in  $Z^0/\gamma \rightarrow q\bar{q}'$  background alone in both channels. Two-photon backgrounds

<sup>8</sup>The ARIADNE events were generated using a different tune of JETSET.



are scaled by a factor of 0.5 or 2, while the  $Z^0/\gamma \rightarrow \tau^+\tau^-$  background is neglected. Shape dependence of the subtracted distribution is estimated by taking the largest variation found when using alternative models for a given source of background, such as HERWIG in place of PYTHIA for the  $Z^0/\gamma$  process, and PYTHIA in place of PHOJET [28] for part of the two-photon process. In the case of the multiplicity distributions, the shape dependence was also tested by shifting the multiplicity by  $\pm 1$  unit. This latter variation accommodates the differences between data and models, and the uncertainty on measured hadronic multiplicity in  $Z^0/\gamma \rightarrow q\bar{q}'$  at  $\sqrt{s} \simeq 182.7$  GeV [29].

The four-fermion background was evaluated by comparing the accepted distributions from two samples of events generated using the grc4f [30] model: one contains the full set of interfering four-fermion diagrams, while the other is restricted to the CC03 set of W pair production diagrams<sup>9</sup>. The same procedure was followed using EXCALIBUR events. A further test of the four-fermion contribution used independent samples of  $W\bar{\nu}_e$ ,  $Z^0Z^0$  and  $Z^0e^+e^-$  final states, generated with the grc4f or PYTHIA Monte Carlo models. The systematic uncertainty from the four-fermion background was taken to be the largest deviation seen from the results obtained using grc4f.

Since most of the Monte Carlo samples used in the study were generated at  $\sqrt{s} = 183$  GeV while the data were taken at various centre-of-mass energies between  $\sim 182$  and 184 GeV, the analysis was repeated using  $W^+W^-$  samples generated at 182 GeV and 184 GeV. The larger effect quantifies the dependence of the analysis on the choice of centre-of-mass energy.

To estimate the sensitivity of the results to the unfolding procedure, the dispersions of the multiplicity distributions and the mean values  $\langle n_{\text{ch}}^{4q} \rangle$ ,  $\langle n_{\text{ch}}^{\text{qq}\ell\nu} \rangle$ ,  $\langle x_p^{\text{qq}\ell\nu} \rangle$ ,  $\langle x_p^{4q} \rangle$ ,  $\langle 1 - T^{4q} \rangle$  and  $\langle |y^{4q}| \rangle$  were each evaluated by applying a single correction factor to each of the uncorrected values, rather than using the methods described in Section 3. This correction is the ratio of the KORALW prediction without detector simulation or initial state radiation, to the corresponding prediction for the same observable when these two effects are included. The change in the corrected value gives an estimate of the systematic error due to the unfolding process.

As a final test, the analysis was repeated using additional event selection criteria, based on the probability obtained from kinematic fits. These required energy and momentum conservation and constrained the masses of the two W boson candidates to be equal. Consistent results were obtained and no additional systematic contributions were assigned.

## 6 Results

The measurements of the mean charged particle multiplicities, fragmentation functions, and their associated differences, corrected to the hadron level, are:

$$\begin{aligned}
\langle n_{\text{ch}}^{4q} \rangle &= 39.4 \pm 0.5 \pm 0.6 \\
\langle n_{\text{ch}}^{\text{qq}\ell\nu} \rangle &= 19.3 \pm 0.3 \pm 0.3 \\
\Delta \langle n_{\text{ch}} \rangle &= +0.7 \pm 0.8 \pm 0.6 \\
\langle x_p^{4q} \rangle &= (3.16 \pm 0.05 \pm 0.03) \times 10^{-2} \\
\langle x_p^{\text{qq}\ell\nu} \rangle &= (3.25 \pm 0.07 \pm 0.04) \times 10^{-2} \\
\Delta \langle x_p \rangle &= (-0.09 \pm 0.09 \pm 0.05) \times 10^{-2}
\end{aligned}$$

---

<sup>9</sup>The W pair production diagrams, *i.e.*  $t$ -channel  $\nu_e$  exchange and  $s$ -channel  $Z^0/\gamma$  exchange, are referred to as ‘‘CC03’’, following the notation of Ref. [13], p. 11.

where in each case the first uncertainty is statistical and the second systematic. Similarly corrected measurements of  $\langle |y^{4q}| \rangle$ ,  $\langle 1 - T^{4q} \rangle$  and the dispersions of the charged particle multiplicity distributions, are also presented in the upper part of Table 3.

These results may be compared with the predictions from various Monte Carlo models, with and without reconnection effects, given in the lower part of Table 3. The predictions of the Ellis-Geiger model in VNI are markedly different from data and other models. The mean thrust indicates that the events are more spherical than data, the momentum spectrum is significantly softer than data, and the mean charged particle multiplicities are significantly higher than in data. Although VNI predicts a much softer momentum spectrum and higher charged multiplicity than data, the behaviour is similar in both  $q\bar{q}'q\bar{q}'$  and  $q\bar{q}'\ell\bar{\nu}_\ell$  channels.

Good agreement is found between the data and the standard QCD models, with the exception of HERWIG as discussed in Section 3. The higher value of  $\langle n_{\text{ch}}^{4q} \rangle$  measured in data than predicted by models can be inferred from the uncorrected multiplicity distribution of Figure 1(a), where a shift of approximately one unit relative to the corresponding predictions from KORALW and ARIADNE may be seen. The  $W^+W^- \rightarrow q\bar{q}'\ell\bar{\nu}_\ell$  data are in good agreement with these models. This difference of approximately one unit in multiplicity is reflected in the final  $\Delta\langle n_{\text{ch}} \rangle$  obtained for the data.

It is interesting to note that at the current precision, the mean charged particle multiplicity of a single hadronic W decay ( $\langle n_{\text{ch}}^{\text{qq}\ell\nu} \rangle$  or  $\langle n_{\text{ch}}^{4q} \rangle / 2$ ) is consistent with that of approximately 19.5 units predicted for  $Z^0/\gamma \rightarrow q\bar{q}'$  at  $\sqrt{s} \simeq M_W$ , despite the different flavour composition expected in the two cases<sup>10</sup>. The predicted multiplicity is obtained from a fit [21] to the NLLA QCD calculation for the energy evolution of the charged particle multiplicity [31], using data between 12 GeV and 133 GeV.

The difference in mean charged multiplicities in hadronic W decays in  $q\bar{q}'q\bar{q}'$  and  $q\bar{q}'\ell\bar{\nu}_\ell$  events,  $\Delta\langle n_{\text{ch}} \rangle$ , is found to be consistent with zero at the current level of statistical precision. The dispersions in these two channels, which should be related by a factor  $\sqrt{2}$  in the case where two hadronically decaying W bosons in a given event are independent of each other, are also found to be consistent with each other. Similarly, the measurements of the mean scaled charged particle momenta are consistent in the two channels. In contrast, the colour reconnection models predict non-zero values of  $\Delta\langle n_{\text{ch}} \rangle$  and  $\Delta\langle x_p \rangle$ , as shown in Table 3. The largest effects are seen for the AR 3 model which is the least consistent with the measurements of  $\Delta\langle n_{\text{ch}} \rangle$  and  $\Delta\langle x_p \rangle$ .

Figures 3(a) and (b) show the corrected fragmentation functions for the  $W^+W^- \rightarrow q\bar{q}'q\bar{q}'$  and  $W^+W^- \rightarrow q\bar{q}'\ell\bar{\nu}_\ell$  channels, together with predictions from the KORALW, HERWIG, AR 3 and VNI models. Most models are in good agreement within statistical uncertainties in both cases. An alternative measurement of the mean charged multiplicity may be obtained from the integral of the fragmentation function. The values determined in this way are  $\langle n_{\text{ch}}^{4q} \rangle = 39.5 \pm 0.9$  and  $\langle n_{\text{ch}}^{\text{qq}\ell\nu} \rangle = 19.3 \pm 0.5$ , where the errors given are combined statistical and systematic uncertainties. Figure 3(c) shows the ratio of the  $x_p^{4q}$  distribution to twice the  $x_p^{\text{qq}\ell\nu}$  distribution for low particle momenta,  $x_p < 0.2$ . There is no significant discrepancy between any of the viable reconnection models and data. Although the behaviour of the AR 3 model indicates differences between the two channels in the low momentum region where the effects of colour reconnection are expected to be enhanced, there no indication that the data show such a tendency.

The corrected rapidity distribution for  $W^+W^- \rightarrow q\bar{q}'q\bar{q}'$  events,  $|y|$  is shown in Figure 4, together with the predictions of various Monte Carlo models. To focus attention on the shape of the distributions, the integrals of the model predictions have been normalised to the measured  $\langle n_{\text{ch}}^{4q} \rangle$ . All of the

<sup>10</sup>The different flavour composition is predicted to lower the charged particle multiplicity of a single hadronic W decay by  $\sim 0.6$  units relative to  $Z^0/\gamma \rightarrow q\bar{q}'$ .

viable models provide a good description of the data over the entire range measured.

## 7 Estimated effect on $M_W$ measurement

The effect predicted by each model of colour reconnection on the OPAL measurement of  $M_W$  in the  $W^+W^- \rightarrow q\bar{q}'q\bar{q}'$  channel was investigated by analysing Monte Carlo  $W^+W^- \rightarrow q\bar{q}'q\bar{q}'$  events, with simulation of the OPAL detector, as if they were data. In each selected event, three kinematic fits are performed corresponding to the possible jet-jet pairings, and further criteria are used to select up to two reconstructed masses per event,  $m_{\text{rec}}$ , as described in the accompanying paper [22].

For each model a possible shift in the measured mass was estimated in three ways. In the first method, a distribution of the event-by-event difference between  $m_{\text{rec}}$  and  $m_{\text{true}}$  was formed, where  $m_{\text{true}}$  is defined as the average of the generated  $W^+$  and  $W^-$  masses. Following the Breit-Wigner fitting analysis of [22], up to two values of  $(m_{\text{rec}} - m_{\text{true}})$  may enter the distribution, depending upon their relative and absolute kinematic fit probabilities. Events admitted to the distribution are required to have radiated less than 0.1 GeV of energy into initial state photons. The shift is estimated from the truncated mean, using a range of  $\pm 3$  GeV. The results of this procedure are given in Table 4 in the column “Method 1a”. A variant of this method, which accounts for possible biases in the mass reconstruction in the non-reconnected samples, defines the colour reconnection effect as the difference between the means in the corresponding reconnected and non-reconnected samples. The results are given in column “Method 1b”.

In the second method, the reweighting analysis used to determine the principal result of [22] was applied to each sample of simulated events, giving a fitted mass,  $M_{\text{fit}}$ . Assuming that this procedure does not introduce any significant bias, the difference between  $M_{\text{fit}}$  and the input  $M_W$  value in the models is taken to be the change in measured  $M_W$  due to colour reconnection. The results of this procedure are given in Table 4 in column “Method 2a”. The column “Method 2b” presents analogous results to Method 1b.

It can be seen that the changes predicted for the non-reconnection models are small and consistent with zero. In contrast, a significant difference is visible for the ARIADNE models, while effects for the Sjöstrand-Khoze models are less pronounced. The largest change in  $M_W$  is seen in the model AR 3 which also predicts the most significant change in  $\Delta\langle n_{\text{ch}} \rangle$ . This model is disfavoured theoretically as noted in Section 4, and experimentally by measurements presented in this letter. Therefore, this model is not used to estimate possible systematic effects on  $M_W$  measurements.

The individual biases of the admissible models are used to estimate the influence which colour reconnection may have on measurements of  $M_W$ . Consistent results are obtained in the three methods. Although Method 1b is the more statistically precise procedure, the overall systematic uncertainty is taken from Method 2b, which accounts explicitly for possible biases inherent in the actual procedure with which  $M_W$  is extracted from data. The largest individual effect is seen from the AR 2 model, with a value of 49 MeV. This is therefore assigned as the current estimate of the systematic uncertainty associated with colour reconnection effects on OPAL measurements of  $M_W$ .

## 8 Conclusions

The  $W^+W^-$  event properties presented here are in good agreement with expectations of standard QCD models. A 10% reduction in  $\langle n_{\text{ch}}^{4q} \rangle$  as predicted by Ellis and Geiger [12] is not supported by data. This difference in the charged multiplicity is not reproduced by the Monte Carlo program VNI in which the Ellis-Geiger model is implemented. The current implementation of the Ellis-Geiger model is excluded by the measured event shape data and therefore is not used in estimating the systematic uncertainty on  $M_W$  from colour reconnection.

Studies of reconnection phenomena implemented with the ARIADNE and PYTHIA models show that changes up to approximately 3% may be expected in  $\langle n_{\text{ch}}^{4q} \rangle$  and  $\langle x_p^{4q} \rangle$ . Defining  $\Delta\langle n_{\text{ch}} \rangle$  and  $\Delta\langle x_p \rangle$  using data alone provides a model independent test of possible reconnection effects. The maximum shifts in these variables predicted by the models considered are at the level 1–2 standard deviations for the current data. There is no indication of the effects of colour reconnection on these observables at the current level of statistical precision.

The effect of colour reconnection on measurements of  $M_W$  is estimated using the Sjöstrand-Khoze and ARIADNE Monte Carlo models of colour reconnection which are theoretically admissible and consistent with the currently available data. A model dependent estimate of  $\Delta M_W = \pm 49$  MeV is currently assigned to the possible influence that colour reconnection may have on  $M_W$  measurements in the  $W^+W^- \rightarrow q\bar{q}'q\bar{q}'$  channel.

## Acknowledgements

We thank Klaus Geiger for his help and support with the computer program VNI, and note with sorrow his tragic death on 2 September 1998.

We particularly wish to thank the SL Division for the efficient operation of the LEP accelerator at all energies and for their continuing close cooperation with our experimental group. We thank our colleagues from CEA, DAPNIA/SPP, CE-Saclay for their efforts over the years on the time-of-flight and trigger systems which we continue to use. In addition to the support staff at our own institutions we are pleased to acknowledge the

Department of Energy, USA,

National Science Foundation, USA,

Particle Physics and Astronomy Research Council, UK,

Natural Sciences and Engineering Research Council, Canada,

Israel Science Foundation, administered by the Israel Academy of Science and Humanities,

Minerva Gesellschaft,

Benozziyo Center for High Energy Physics,

Japanese Ministry of Education, Science and Culture (the Monbusho) and a grant under the Monbusho

International Science Research Program,

Japanese Society for the Promotion of Science (JSPS),

German Israeli Bi-national Science Foundation (GIF),

Bundesministerium für Bildung, Wissenschaft, Forschung und Technologie, Germany,

National Research Council of Canada,

Research Corporation, USA,

Hungarian Foundation for Scientific Research, OTKA T-016660, T023793 and OTKA F-023259.

## References

- [1] G. Gustafson, U. Petterson and P.M. Zerwas, Phys. Lett. **B209** (1988) 90.
- [2] T. Sjöstrand and V.A. Khoze, Z. Phys. **C62** (1994) 281; Phys. Rev. Lett. **72** (1994) 28.
- [3] T. Sjöstrand, Comput. Phys. Commun. **82** (1994) 74.
- [4] G. Gustafson, J. Häkkinen, Z. Phys. **C64** (1994) 659;  
C. Friberg, G. Gustafson and J. Häkkinen, Nucl. Phys. **B490** (1997) 289.
- [5] L. Lönnblad, Z. Phys. **C70** (1996) 107.
- [6] L. Lönnblad, Comput. Phys. Commun. **71** (1992) 15.
- [7] G. Marchesini *et al.*, Comput. Phys. Commun. **67** (1992) 465.
- [8] J. Ellis and K. Geiger, Phys. Rev. **D54** (1996) 1967.
- [9] K. Geiger, Comput. Phys. Commun. **104** (1997) 70.
- [10] J. Häkkinen and M. Ringner, Eur. Phys. J. **C5** (1998) 275.
- [11] A. Ballestrero *et al.*, J. Phys. G: Nucl. Part. Phys. **24** (1998) 365.
- [12] J. Ellis and K. Geiger, Phys. Lett. **B404** (1997) 230.
- [13] Proceedings of CERN LEP2 Workshop, CERN 96-01, Vol. 2, p. 159,  
eds. G. Altarelli, T. Sjöstrand and F. Zwirner, February 1996.
- [14] B.R. Webber, J. Phys. G: Nucl. Part. Phys. **24** (1998) 287.
- [15] OPAL Collaboration, K. Ahmet *et al.*, Nucl. Instr. Meth. **A305** (1991) 275;  
B.E. Anderson *et al.*, IEEE Transactions on Nuclear Science, **41** (1994) 845;  
S. Anderson *et al.*, Nucl. Instr. Meth. **A403** (1998) 326.
- [16] OPAL Collaboration, K. Ackerstaff *et al.*, Eur. Phys. J. **C6** (1999) 1.
- [17] LEP Energy Working Group, A. Blondel *et al.*, *Evaluation of the LEP centre-of-mass energy above the W-pair production threshold*, CERN-SL/98-yyy, paper in preparation.
- [18] OPAL Collaboration, K. Ackerstaff *et al.*, Eur. Phys. J. **C1** (1998) 395.
- [19] OPAL Collaboration, G. Abbiendi *et al.*, CERN-EP/98-167, submitted to Eur. Phys. J. **C**.
- [20] M. Skrzypek *et al.*, Comput. Phys. Commun. **94** (1996) 216;  
M. Skrzypek *et al.*, Phys. Lett. **B372** (1996) 289.
- [21] OPAL Collaboration, G. Alexander *et al.*, Z. Phys. **C72** (1996) 191.
- [22] OPAL Collaboration, G. Abbiendi *et al.*, *Measurement of the W mass and width in  $e^+e^-$  collisions at 183 GeV*, CERN-EP/98-xxx, submitted to Phys. Lett. **B**.
- [23] T. Sjöstrand and V.A. Khoze, *Soft particle spectra as a probe of interconnection effects in hadronic  $W^+W^-$  events*, CERN-TH/98-74,  
`\protect\vrule width0pt\protect\href{http://arxiv.org/abs/hep-ph/9804202}{hep-ph/9804202}`.
- [24] Proceedings of CERN LEP2 Workshop, CERN 96-01, Vol. 1, p. 141,  
eds. G. Altarelli, T. Sjöstrand and F. Zwirner, February 1996.

- [25] ALEPH Collaboration, R. Barate *et al.*, Phys. Rep. **294** (1998) 1.
- [26] F.A. Berends, R. Pittau and R. Kleiss, Comput. Phys. Commun. **85** (1995) 437.
- [27] D. Bardin *et al.*, Nucl. Phys. **B**, Proc. Suppl. **37B** (1994) 148;  
D. Bardin *et al.*, Comput. Phys. Commun. **104** (1997) 161.
- [28] R. Engel and J. Ranft, Phys. Rev. **D54** (1996) 4244;  
R. Engel, Z. Phys. **C66** (1995) 203.
- [29] L3 Collaboration, M. Acciarri *et al.*, *QCD results from studies of hadronic events produced in  $e^+e^-$  annihilations at  $\sqrt{s} = 183$  GeV*, CERN-EP/98-148, to appear in Phys. Lett. **B**.
- [30] J. Fujimoto *et al.*, Comput. Phys. Commun. **100** (1997) 128.
- [31] B.R. Webber, Phys. Lett. **B143** (1984) 501.

Systematic variation	$\langle n_{\text{ch}}^{4\text{q}} \rangle$	$\langle n_{\text{ch}}^{\text{qq}\ell\nu} \rangle$	$\Delta \langle n_{\text{ch}} \rangle$	$D^{4\text{q}}$	$D^{\text{qq}\ell\nu}$	$\Delta D$
W <sup>+</sup> W <sup>-</sup> model	0.14	0.03	0.13	0.13	0.08	0.16
Hadronisation model	0.45	0.21	0.41	0.45	0.31	0.11
Track quality cuts	0.25	0.12	0.25	0.15	0.11	0.08
Background model	0.23	0.05	0.17	0.03	0.02	0.02
Four-fermion background	0.18	0.05	0.08	0.07	0.02	0.06
Centre-of-mass energy	0.01	0.11	0.21	0.06	0.06	0.08
Unfolding procedure	0.12	0.03	0.17	0.07	0.06	0.10
Total	0.62	0.28	0.60	0.51	0.35	0.25

Table 1: Individual contributions to the systematic uncertainties on charged multiplicity related quantities.

Systematic variation	$\langle x_p^{4\text{q}} \rangle$ $\times 10^2$	$\langle x_p^{\text{qq}\ell\nu} \rangle$ $\times 10^2$	$\Delta \langle x_p \rangle$ $\times 10^2$	$\langle 1 - T^{4\text{q}} \rangle$ $\times 10^2$	$\langle  y^{4\text{q}}  \rangle$ $\times 10^2$
W <sup>+</sup> W <sup>-</sup> model	0.012	0.008	0.018	0.11	0.28
Hadronisation model	0.012	0.015	0.019	0.29	0.81
Track quality cuts	0.019	0.018	0.015	0.11	0.31
Background model	0.003	0.006	0.005	0.27	0.96
Four-fermion background	0.011	0.019	0.027	0.08	0.23
Centre-of-mass energy	0.012	0.019	0.018	0.36	0.38
Unfolding procedure	0.002	0.019	0.022	0.68	0.17
Total	0.031	0.042	0.049	0.87	1.4

Table 2: Individual contributions to the systematic uncertainties on the average event properties.

Sample	$P^{\text{reco}}$ (%)	$\langle n_{\text{ch}}^{4\text{q}} \rangle$	$\langle n_{\text{ch}}^{\text{qq}\ell\nu} \rangle$	$\Delta \langle n_{\text{ch}} \rangle$	$D^{4\text{q}}$	$D^{\text{qq}\ell\nu}$	$\Delta D$	$\langle x_p^{4\text{q}} \rangle$ $\times 10^2$	$\langle x_p^{\text{qq}\ell\nu} \rangle$ $\times 10^2$	$\Delta \langle x_p \rangle$ $\times 10^2$	$\langle 1 - T^{4\text{q}} \rangle$	$\langle  y^{4\text{q}}  \rangle$
Data		39.4	19.3	+0.7	8.8	6.1	+0.2	3.16	3.25	-0.09	0.240	1.011
stat.		$\pm 0.5$	$\pm 0.3$	$\pm 0.8$	$\pm 0.3$	$\pm 0.3$	$\pm 0.5$	$\pm 0.05$	$\pm 0.07$	$\pm 0.09$	$\pm 0.015$	$\pm 0.014$
syst.		$\pm 0.6$	$\pm 0.3$	$\pm 0.6$	$\pm 0.5$	$\pm 0.4$	$\pm 0.3$	$\pm 0.03$	$\pm 0.04$	$\pm 0.05$	$\pm 0.009$	$\pm 0.014$
KORALW	0.0	38.78	19.38	+0.01	8.47	6.00	-0.01	3.21	3.21	0.00	0.240	1.009
HERWIG	0.0	37.24	18.63	-0.02	8.65	6.14	-0.03	3.31	3.30	0.01	0.239	1.009
PYTHIA	0.0	38.77	19.39	-0.01	8.49	5.97	+0.05	3.21	3.21	0.00	0.240	1.009
SK I	37.9	38.39	-	-0.38	8.45	-	+0.01	3.25	-	+0.04	0.239	1.015
SK II	22.2	38.59	-	-0.19	8.45	-	+0.01	3.23	-	+0.02	0.240	1.010
SK II'	19.8	38.54	-	-0.24	8.41	-	-0.03	3.23	-	+0.02	0.240	1.011
ARIADNE	0.0	38.47	19.22	+0.04	8.23	5.82	0.00	3.22	3.22	0.00	0.240	1.009
AR 2	51.9	38.31	19.31	-0.31	8.01	5.67	-0.01	3.24	3.21	+0.03	0.239	1.013
AR 3	63.4	37.45	19.17	-0.90	7.96	5.67	-0.05	3.31	3.23	+0.08	0.238	1.024
VNI(blind)	> 0	68.5	35.0	-1.6	14.8	10.6	-0.1	1.80	1.74	-0.06	0.30	0.81
VNI(singlet)	> 0	70.3	34.4	+1.4	15.5	10.7	+0.5	1.76	1.89	-0.13	0.31	0.80

Table 3: Summary of measurements performed, after correction to the hadron level. The predictions from a variety of Monte Carlo models, with and without colour reconnection effects, are also given. The fraction of events in which at least one reconnection has occurred in  $W^+W^- \rightarrow q\bar{q}'q\bar{q}'$  events is indicated by the column,  $P^{\text{reco}}$ . Statistical uncertainties in the Monte Carlo predictions are typically 1–2 units in the least significant digit. In the case of the Sjöstrand-Khoze models which do not include reconnection for  $W^+W^- \rightarrow q\bar{q}'\ell\bar{\nu}_\ell$  events, the predictions from the corresponding “no reconnection” sample (PYTHIA) were used to determine the quantities  $\Delta \langle n_{\text{ch}} \rangle$ ,  $\Delta D$  and  $\Delta \langle x_p \rangle$ .



Model	$M_W$ bias (MeV)			
	Method 1a	Method 1b	Method 2a	Method 2b
KORALW	$-11 \pm 11$	–	$-12 \pm 18$	–
HERWIG	$-13 \pm 9$	–	$-26 \pm 15$	–
PYTHIA	$+2 \pm 9$	–	$+30 \pm 18$	–
SK I	$+43 \pm 9$	$+41 \pm 13$	$+41 \pm 18$	$+11 \pm 25$
SK II	$+1 \pm 9$	$-1 \pm 13$	$+7 \pm 18$	$-23 \pm 25$
SK II'	$+4 \pm 9$	$+2 \pm 13$	$+8 \pm 18$	$-22 \pm 25$
ARIADNE	$-10 \pm 5$	–	$-7 \pm 10$	–
AR 2	$+37 \pm 5$	$+47 \pm 7$	$+42 \pm 10$	$+49 \pm 14$
AR 3	$+100 \pm 10$	$+110 \pm 11$	$+138 \pm 18$	$+145 \pm 21$

Table 4: Predictions for the bias in the measured  $M_W$  from a variety of Monte Carlo models, with and without colour reconnection effects. Simulation of the OPAL detector is included.

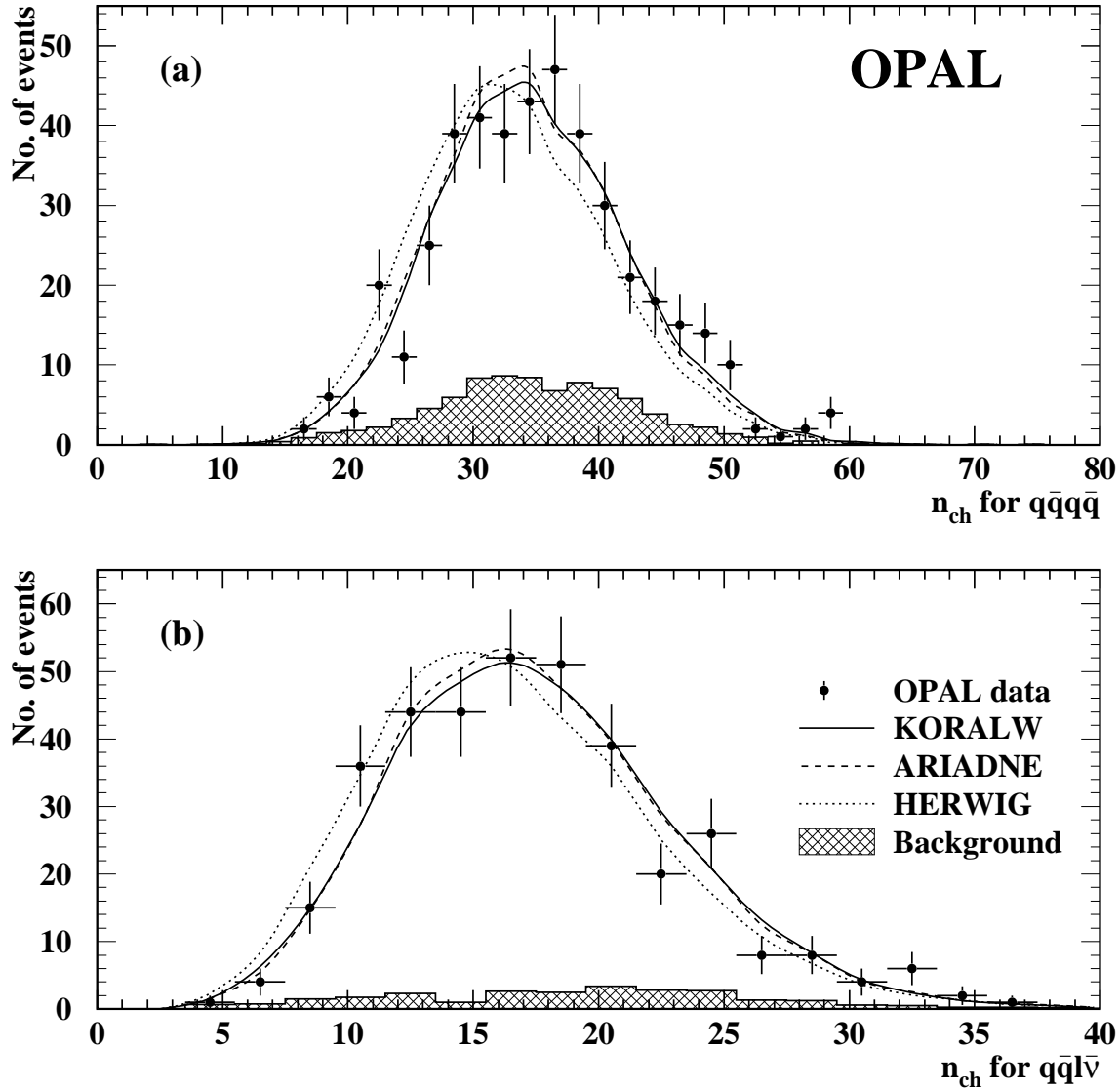


Figure 1: Uncorrected charged multiplicity distributions for (a)  $W^+W^- \rightarrow q\bar{q}'q\bar{q}'$  events and (b) the hadronic part of  $W^+W^- \rightarrow q\bar{q}'l\bar{\nu}_l$  events. Points indicate the data, smooth curves show the expected sum of signal and background contributions for a variety of signal models, and the hatched histogram shows the expected background. Predictions of KORALW, PYTHIA and EXCALIBUR are indistinguishable from one another.

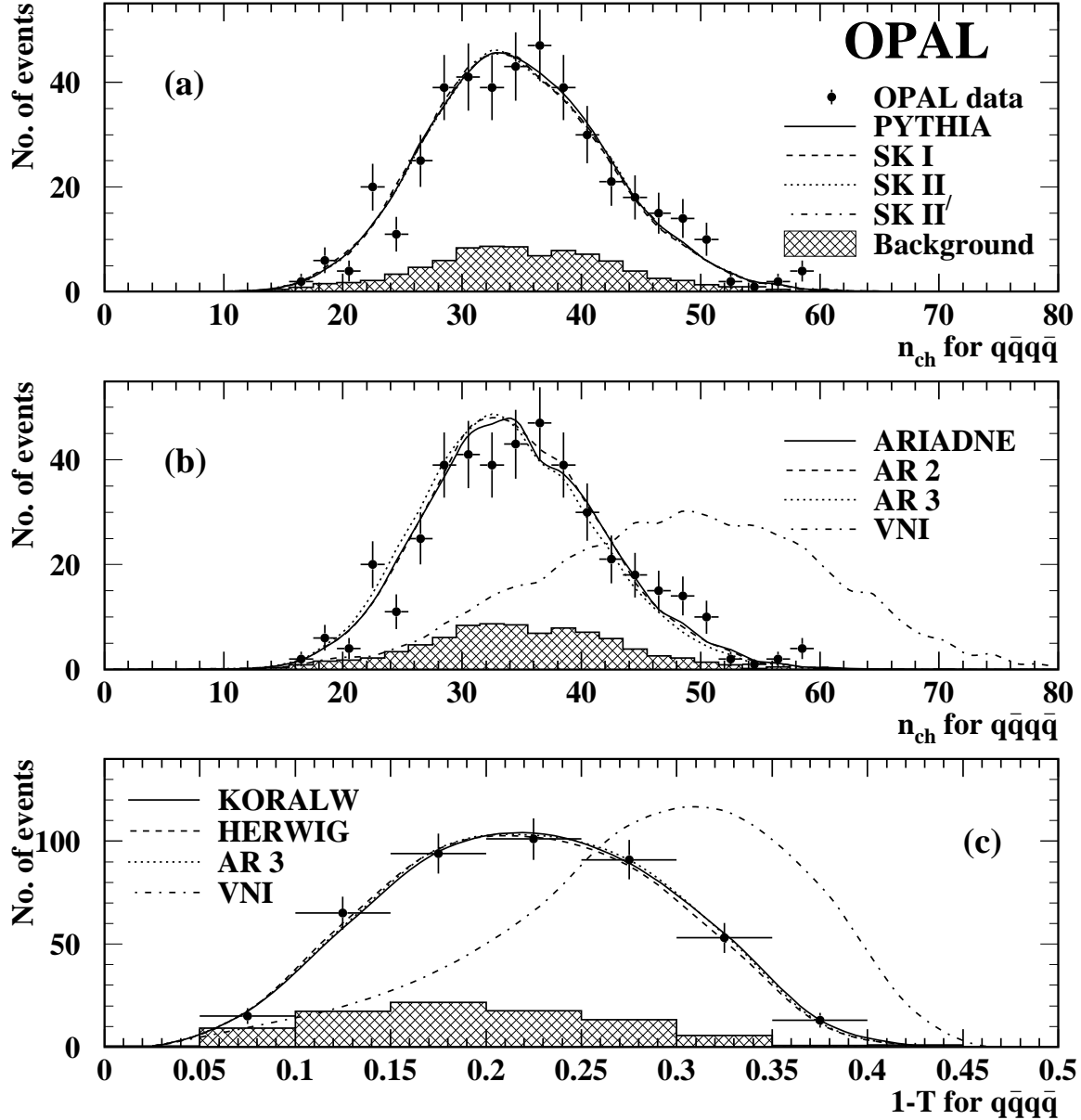


Figure 2: Uncorrected charged multiplicity distributions for  $W^+W^- \rightarrow q\bar{q}'q\bar{q}'$  events, compared with (a) PYTHIA and the three Sjöstrand-Khoze models of colour reconnection, and (b) ARIADNE and Ellis-Geiger (colour blind) models of colour reconnection. Similarly, (c) compares the uncorrected thrust distribution for  $W^+W^- \rightarrow q\bar{q}'q\bar{q}'$  events with a selection of the models, with and without colour reconnection. Points indicate the data, smooth curves show the expected sum of signal and background contributions for a variety of signal models, and the hatched histogram shows the expected background.

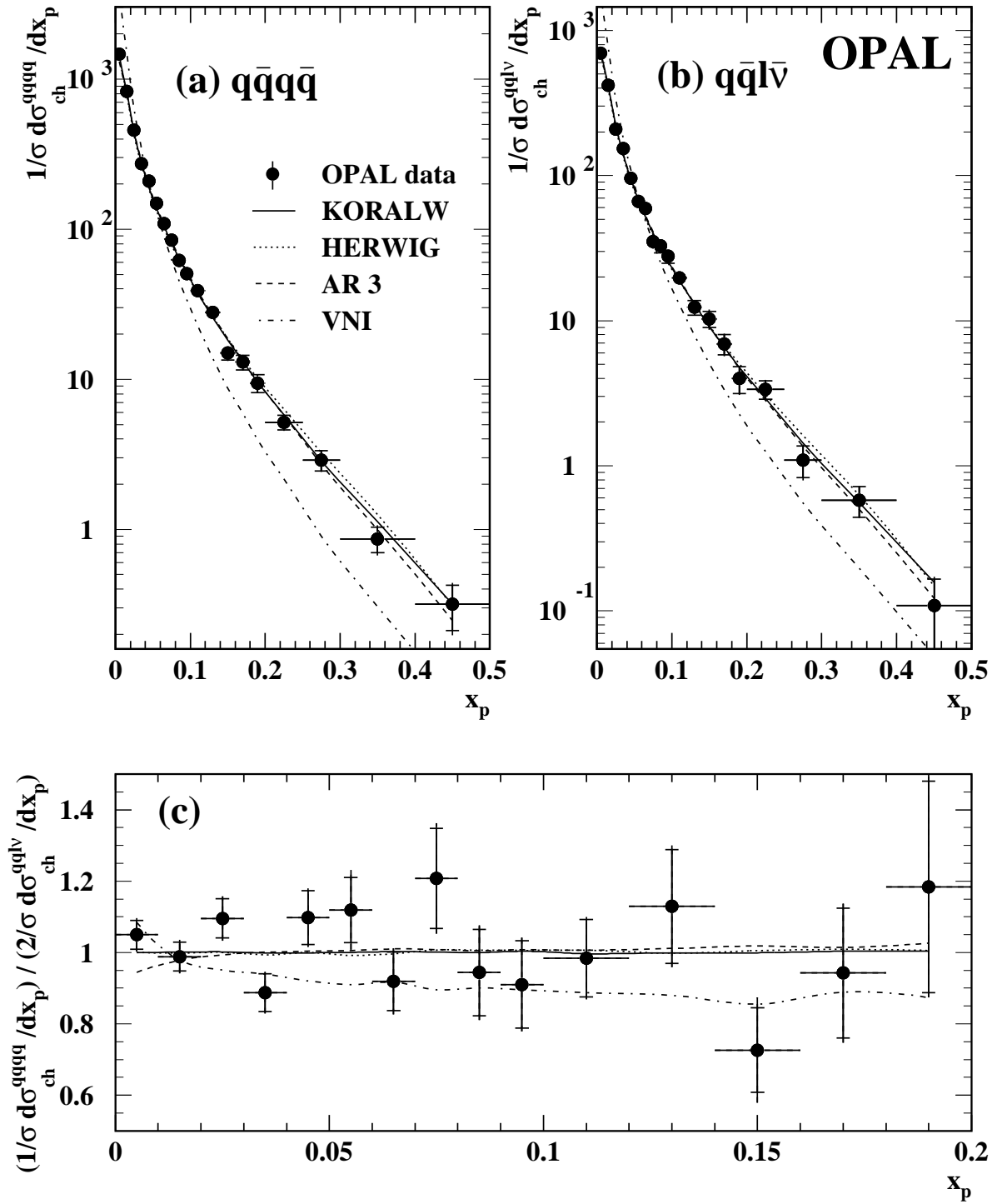


Figure 3: Corrected  $x_p$  distributions for (a)  $W^+W^- \rightarrow q\bar{q}'q\bar{q}'$  events, (b) the hadronic part of  $W^+W^- \rightarrow q\bar{q}'l\bar{\nu}_l$  events and (c) the ratio of the  $W^+W^- \rightarrow q\bar{q}'q\bar{q}'$  distribution to twice the  $W^+W^- \rightarrow q\bar{q}'l\bar{\nu}_l$  distribution. Points indicate the data, with statistical (horizontal bars) and systematic uncertainties added in quadrature. Point to point correlations exist in the systematic uncertainties. Predictions of various Monte Carlo models (with and without colour reconnection) are shown as smooth curves. VNI predictions correspond to the colour singlet variant of the Ellis-Geiger model. Sjöstrand-Khoze and AR 2 models are not shown as they are essentially indistinguishable from KORALW.

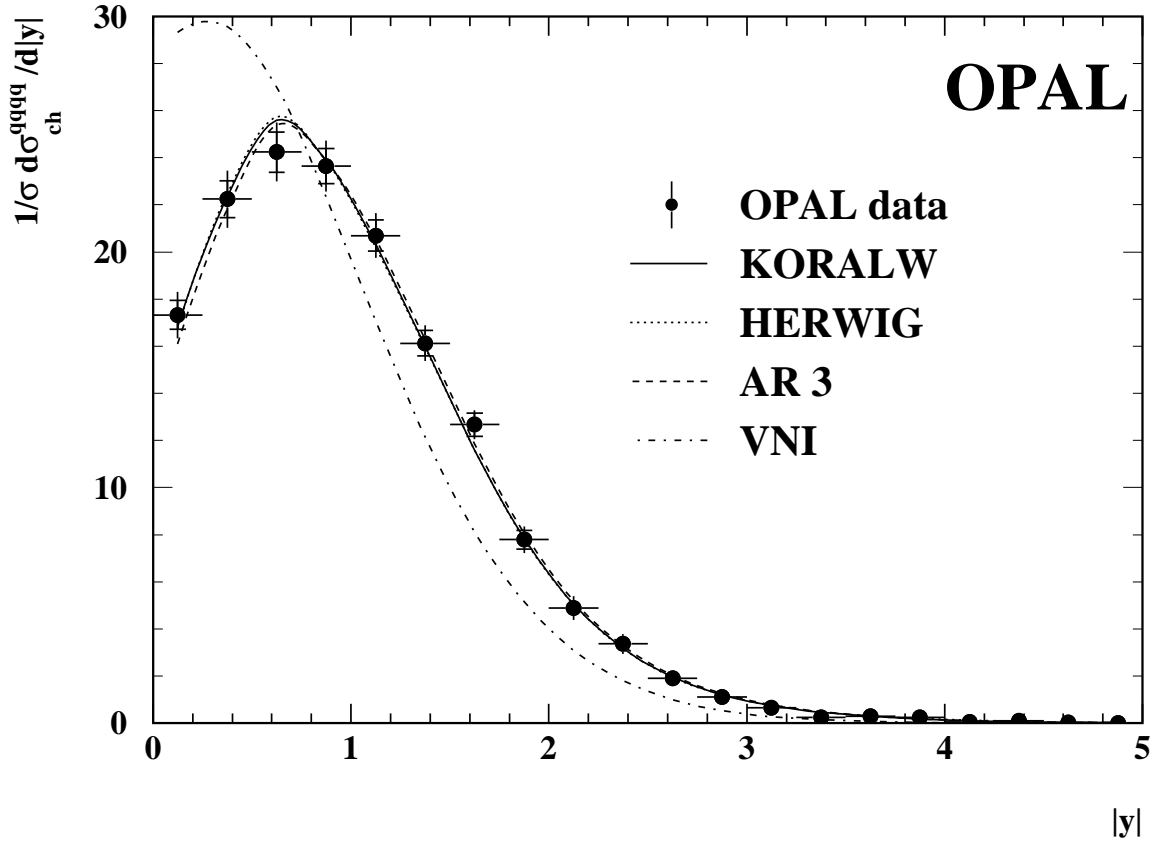


Figure 4: Corrected rapidity distribution for  $W^+W^- \rightarrow q\bar{q}'q\bar{q}'$  events. Points indicate the data, with statistical (horizontal bars) and systematic uncertainties added in quadrature. Point to point correlations exist in the systematic uncertainties. Predictions of various Monte Carlo models (with and without colour reconnection) are shown as smooth curves. VNI predictions correspond to the colour singlet variant of the Ellis-Geiger model. All models are normalised to the measured  $\langle n_{ch}^{4q} \rangle$ . Sjöstrand-Khoze and AR 2 models are not shown as they are essentially indistinguishable from KORALW.